Published in the Slovak Republic
European Journal of Medicine
Has been issued since 2013.
E-ISSN: 2310-3434
2019, 7(2): 68-91

DOI: 10.13187/ejm.2019.2.68
www.ejournal5.com

Articles

Multi-Beam Interference Patterns of Living Sarcoma Cells may be Approximated by a Fractal Julia Set and Rieman Spheres or Fatou Components Decoded as a Siegel Discs

Alexander Bolkhovitinov [a], Viktor Krukowskikh [a], Serge Pankratov [a]

[a] INEPCP (2014, 2016), Moscow, Russian Federation

Abstract

It's well known, that the morphology of a carcinoma cells was studied many a time and oft (on repeated occasions) from the second part of the XX century. But mathematical approximations of such sarcoma cell structures are not very good on the grounds of non-regular semi-chaotic elements in morphogenesis and morphology of cancer cells. Many approximations in sarcoma oncology works are not applying for cell morphology as is, despite the fact of good morphological representation of sarcoma cells in different microscopic and specific-staining methods. Our work is a first work where the multi-beam interference patterns of living sarcoma cells are approximated by a fractal Julia set and Fatou components known as a Siegel discs.

Keywords: sarcoma, oncomorphology, interference microscopy, multi-beam interference, Fatou components, Siegel discs, Riman spheres, Julia set.

1. Introduction

1. Why the carcinoma cell is optimal object for analytical morphology?

It's well known, that the morphology of a carcinoma cells was studied many a time and oft (on repeated occasions) from the second part of the XX century. They were analyzed not only in static, but also in dynamic (kinetic) reaction conditions, which may be applied as potential therapeutic agents, including a respiration and morphology of sarcoma cells exposed to liquid nitrogen (Hodapp et al., 1952).

We can separate physical or physiotherapeutic and chemical or chemotherapeutic agents (Prince, 1962) of this reaction studies into multiple dimensions of multi-descriptor scores (or manifolds):

I. channelome-mediated agent pulls (Civitelli et al., 1992);

II. second messenger pulls (for example, cyclic adenosine monophosphate = 3',5'-cyclic adenosine monophosphate, which is equivalent to cAMP, cyclic AMP, in abbreviations) (Mitchell et al., 1978));

III. cytoskeleton-associated agent pulls (for example – ABP-assisted pulls [Actin-Binding Protein], in particular – vinculin* phosphorylation pulls (Kellie et al., 1986);

* By definitions: 1) vinculin is a membrane-cytoskeletal protein in focal adhesion plaques that is involved in linkage of integrin adhesion molecules to the actin cytoskeleton; 2) vinculin is a cytoskeletal protein associated with cell-cell and cell-matrix junctions, where it is thought to function as one of several interacting proteins involved in anchoring F-actin to the membrane; 3) vinculin is actin binding protein localized in focal

IV. dose dependent effect pulls (for some agents, such as sodium butyrate), including inhibition of proliferation pulls, differentiation induction and repression induction (repression of gene expression) pulls (Altenburg et al., 1976);
V. sarcoma growth factors and their derivatives or mimetics (Keski-Oja et al., 1980; Tokuyama and Tokuyama, 1989);
VI. pulls of clonal factors (Earle, 1975);
VII. mitotropic and nucleotropic agents (Seegers et al., 1992);
VIII. virological agent pulls (Smidová et al., 1968; Altenburg et al., 1976);
IX. pulls of oncogenic agents *sensu stricto* (Chaturvedi, 2013);
X. snake venom cytotoxin pulls (Pate et al., 1969).

But mathematical approximations of such sarcoma cell structures are not very good on the grounds of non-regular semi-chaotic elements in morphogenesis and morphology of cancer cells. Many approximations in sarcoma oncology works are not applying for cell morphology as is (Svoboda and Hasek, 1956), despite the fact of good morphological representation of sarcoma cells in different microscopic and specific-staining methods. In different years for sarcoma oncology studies many different microscopic and specific-staining methods was applied. Among them were noted:

A. electron microscopy (Gandzii, 1956; Yasuzumi et al., 1960; Luse, 1960; Driessens et al., 1964; Kubo et al., 1969; Courington and Vogt, 1967; Rice et al., 1973; Waldo, 1979; Kukuté and Smirnova, 1981; Choux et al., 1981; Kanaya et al., 1985; Husain and Nguyen, 1995; Marquart, 2006)
B. combined electron and light microscopy (Weinberger and Banfield, 1965; Fabrizio and Cottrell, 1972; Fj et al., 1975; Varela and Diazflores, 1977; Waldo et al., 1983; Akerman, 1988; Åkerman et al., 1988; Beziat et al, 1989);
C. comparative scanning electron microscopy and transmission electron microscopy (Llombart-Bosch and Peydro-Olaya, 1983)
D. mass determination of sarcoma virus virions by scanning transmission electron microscopy (Vogt and Simon, 1999);
E. cryo-electron microscopy (Briggs et al., 2006);
F. immunoelectron microscopy (Aoki et al., 1973; Houston, 1974; Hiraki et al., 1974; Kawauchi, 1995; Becker et al., 1991);
G. comparative electron microscopic and immunohistochemical studies (Mukai et al., 1983; Oord et al., 1986; Welch, et al., 1986; Nonomura et al., 1988; Nanomuna, 1988; Pettinato et al., 1989; Nishio et al., 2003);
H. comparative light-scattering spectroscopy and electron microscopy for determination of hydrodynamic radiuses of viruses in sarcoma cells (Salmeen et al., 1976;
I. electron microscopy of viruses in sarcoma cells (Nishimi et al., 1961; Hanaichi et al., 1975; Orenstein et al., 1997; Said et al., 1997);
J. electron microscopy of nucleic acids of sarcoma cells (Guntaka et al., 1976; Murti et al., 1981);
K. conventional or light microscopy (Siegler, 1970; Ackerman, 1979; Amazon and Rywlin, 1979; Tsokos et al., 1988);
L. correlation studies between microscopy data, magnetic resonance imaging data and positron emission tomography data [or two-photon emission tomography data, which are equivalents] (Plowman et al., 2016);
M. phase contrast microscopy (Ludford and Smiles, 1950; Kato and Makino, 1962; Veselý and Pluta, 1972);
N. florescence microscopy (Dorfman, 1962), including epiluminescent microscopy (Krischer et al., 1999);
O. ultraviolet microscopy (Roe and King, 1950; Zhudina and Shalumovich, 1969;
P. in vivo reflectance confocal microscopy (Grazziotin et al., 2010; Paganelli et al., 2018);
Q. structured illumination microscopy (Fu et al., 2016);

adhesions and cell-cell junctions; 4) vinculin is tyrosine phosphorylated in platelets spread on fibrinogen and that the phosphorylation is Src kinases dependent.

R. interference microsopy and quantitative cytology / cytopathology based on this technique, including multiple-beam interference microscopy and similar analytical protocols (Mellors et al., 1953).

2. Why interference microscopy is optimal micro-technique for analytical morphology?

Unfortunately, despite this fact (particularly, despite the quantitative character of multiple-beam interference microscopy, consequently, the quantitative character of interference cytometric and cytopathological data), as a general rule interference microscopy are not usable as a wild-field histological method for carcinoma cell morphology visualization, detection and quantification. It is not very good simplification of research protocols and microdiagnostic approaches, because the photometric methods for the measurement of the organic mass of cells, cell components (including sets of chromosomes) by multiple beam interference microscopy are not only possible, but also they are very effective (Melors, 1953, 1954)!

Multiple-beam interference microscopy was developed initially not only as a technique for material science and metallography (Faust, 1952), but from the third quarter of the XX century they was applied predominantly for metal structure analysis (Tolansky, 1970; Richardson, 1972) and (much later) for liquid crystal measurements, based on the phase retardation principles (Chernyaev et al., 2008). Multiple-beam interference microscopy was reborn in 2000th, when multiple beam interference confocal microscopy was designed and implemented in cell biology laboratories (Joshi and Medina, 2000; Joshi and Medina, 2000b), including biophysical departments, where some effects of an electric field on the motility of cells was examined by multiple-beam interference microscopy techniques (Joshi et al., 2001). Detection, dynamical imaging and kinetics of sub-micron organelles of specialized cells (for example – chondrocytes) were implemented by multiple beam interference microscopy in 2004 (Joshi et al., 2004). Diffential interference phase contrast microscopy using multiple beam shearing interferometry for bio-imaging was applied in 2006 (Roy et al., 2006). Capturing and sorting of multiple cells by polarization-controlled three-beam interference was realized in 2016 (Hou et al., 2016). But such methods were not applied for carcinoma cells.

3. What kind of interference microscopy is optimal for the target cells?

Everyone would very much like to eliminate this omission, because methods of interference microscopy and by interference phase microscopy of cancer cells were developed from 1960th (Sandritter et al., 1960; Hirst, 1961) and very good developed to date or by now (in frames of spatial light interference microscopy (Majeed et al., 2015, 2016), differential interference contrast microscopy assisted by nanoparticles (Sun et al., 2008, 2010), reflection interference contrast microscopy (Matsuzaki et al, 2016)). It is a very specialized branch of the general trend of interference microscopy of living cells, provided in different techniques, such as:

1) digital holographic interferention microscopy (Kizilova et al., 2010);
2) spatial light interference microscopy (Babacan et al., 2011; Popescu and Wang, 2012), including deconvolved spatial light interference microscopy for live cell imaging (Haldar et al., 2011);
3) interference reflection microscopy (Gingell and Todd, 1979; Verschueren, 1985), including quantitative reflection interference contrast microscopy or RICM (Schindl et al., 1995; Usson et al., 1997; Holt et al., 2008; Limozin and Sengupta, 2009);
4) fluorescence interference-contrast microscopy (Braun and Fromherz, 1997);
5) phase-shifting interference microscopy (Dunn and Zicha, 1993);
6) correlational mapping between interference-reflexion and indirect-immunofluorescence microscopy photoregistrograms (Wehland et al., 1979);
7) laser interference microscopy with volumetric and cytorefractometric measurements (Yusipovich et al., 2011) and coherent phase microscopy (Tychinsky and Tikhonov, 2010a; Tychinsky and Tikhonov, 2010b);
8) phase-modulation laser interference microscopy (Brazhe et al., 2008);
9) interference microscopy under double-wavelet analysis (Sosnovtseva et al., 2005);
10) dual-interference-channel quantitative-phase microscopy (Shaked et al., 2009);
11) scanning angle interference microscopy (Paszek et al., 2012);

12) Nomarski differential interference contrast microscopy (Geissinger and Bond, 1971; Geissinger and Duitschaever, 1971) and other (for example – Pluto DIC) differential interference contrast microscopy techniques (Falimirski et al., 2007);

13) total internal reflection aqueous fluorescence overcomes a basic ambiguity of interference reflection microscopy (Todd et al., 1988); etc.

4. Why multiple beam interference microscopy is informative source?

It's known, that the multiple beam interference may be used for discrete signal transmission with small noise levels (Bhardwaj et al., 2017; Hibino and Takatsuji, 2002). Multiple-beam interference effects in Fabry-Perot interferometer with small wedge between mirrors, deriving expressions for light beams path, were researched in 1970th not only in USA, but also in USSR (Koniukhov, 1971). Mechano-optical transductors / sensors based on multiple-beam interference were introduced for optical waveguide measurements in XXI century (El-Diastry, 2001), but their physical and technical principles were developed in XX century, where the Barakat group was started the project on the GRIN optical waveguides (Barakat et al., 1985, 1988, 2001), despite the fact, that the first Barakat works for multiple beam interference studies were published in 1960th (Barakat and Abouzakhm, 1985; Barakat et al., 1965). Earliest works on multiple beam interference fringes and their applications were published from 1940th to 1960th (Tolansky, 1945; Brossel, 1946; Tolansky and Barakat, 1950; Bruce, 1951; Glauert, 1951; Smith, F. D. 1952; Tolansky and Emara, 1955; Hargreaves, 1963; Burnett, 1965; Herriott, 1965, 1966; Fulinska, 1966). Some very beautiful works were published in 1970th (Roberge and Boivin, 1971; Koppelmann, 1972, 1974; Koppelmann and Vosskuhl, 1973) and 1980th (El-Dehemy et al., 1981; Baumbach et al, 1989). Fist articles by Tolansky were republished in 1990th – 2000th in "SPIE milestone series" (Tolansky, 1991, 2000). Many interesting applications for multiple beam interference fringes were provided in 1990th – 2000th (Shao-po, 1999; Tadmor et al., 2003; Abdelsalam et al., 2010; Hamza et al., 2010; El-Hennawi et al., 2012).

2. Relevance

Different types of cells may be measured and quantitative or semi-quantitative visualized by different methods of interference microscopy (Mellors, 1953; Barer and Joseph, 1957; Dunn, Zicha, 1994). Examples include:

- calculation of lignin concentration and porosity of cell-wall regions by interference microscopy (Boutelje, 1972; Donaldson, 1985);
- dry mass and cell area measurements (Goldacre et al., 1957; Lee at al., 1960);
- cell-substrate interactions in amoeboid locomotion (King et al., 1983);
- interaction between intracellular vacuoles and the cell surface (Gingell, 1982);
- growth cone interactions with cell and substrate adhesion molecules of cells (Drazba et al., 1997);
- visualization of red cell membranes (Miller and Dvorak, 1973);
- bacterial cell identification in DIC interference contrast microscopy in label-free conditions (Obara et al., 2013);
- radiation dose effect analysis (Lee and Richards, 1964);
- comparative analysis of epithelial cells (Pappelis et al., 1976);
- real time 3D and "4D" imaging of cells (Salmon et al., 1998; Li et al., 2007; Tsunoda et al., 2008), from yeast cells to cancer cels.

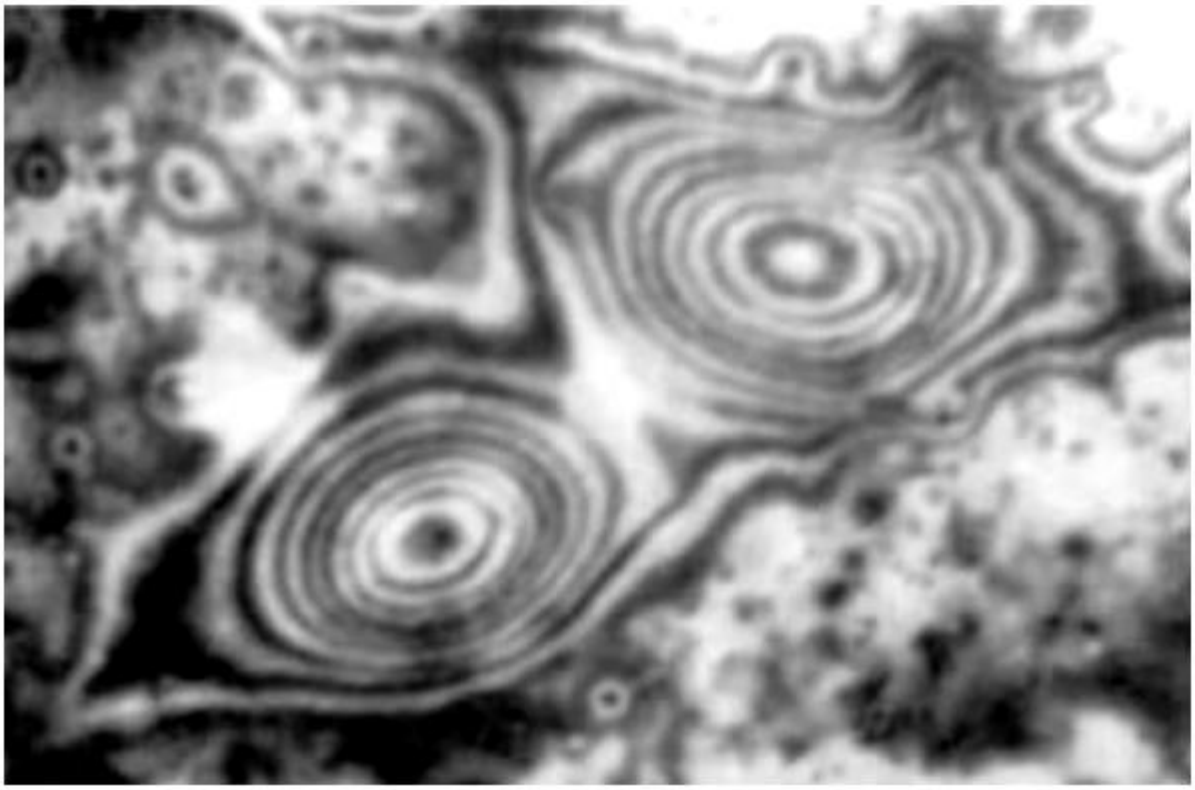

Fig. 1. Multiple beam interference image of living sarcoma cells in a tissue culture

3. Materials and methods

It has been known that biological membranes as thin films are characterized by multiple-beam interference and, consequently, can be directly detected using multiple-beam interference microscopy. Multiple beam interference microscopy patterns of membranous cellular structures with different surface tension levels are different from the standard optical images of these objects. This follows at once from physical considerations. Thin-film interference occurs when the incident light waves reflected by the upper and lower boundaries of the membrane cell film interfere with one another to form a new wave.

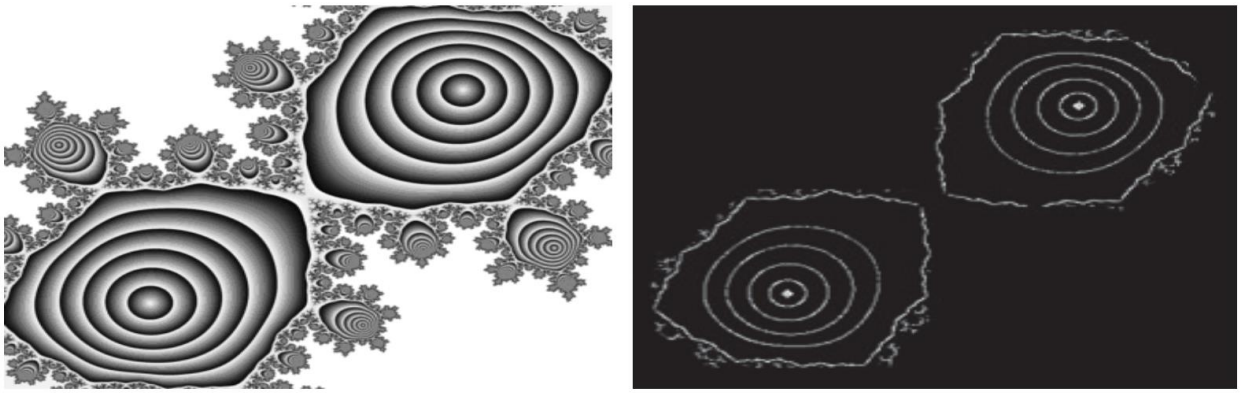

A B

Fig. 2. A fractal Julia set with a Siegel disc (A) and a filled Julia set for the golden mean rotation number with the the Siegel disc and some orbits inside (B)

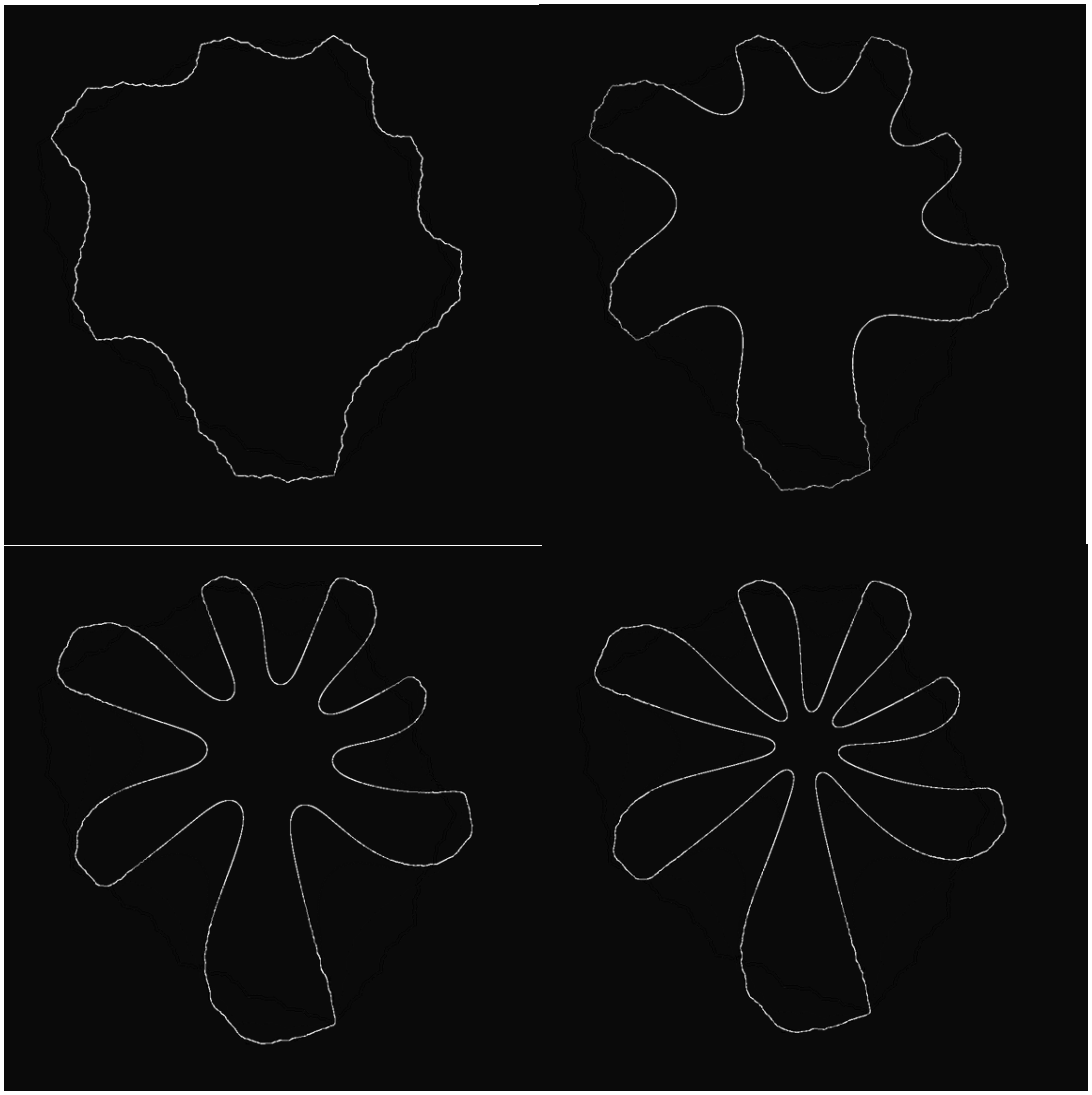

Fig. 3. Infolding Siegel disc near 2/7

4. Results

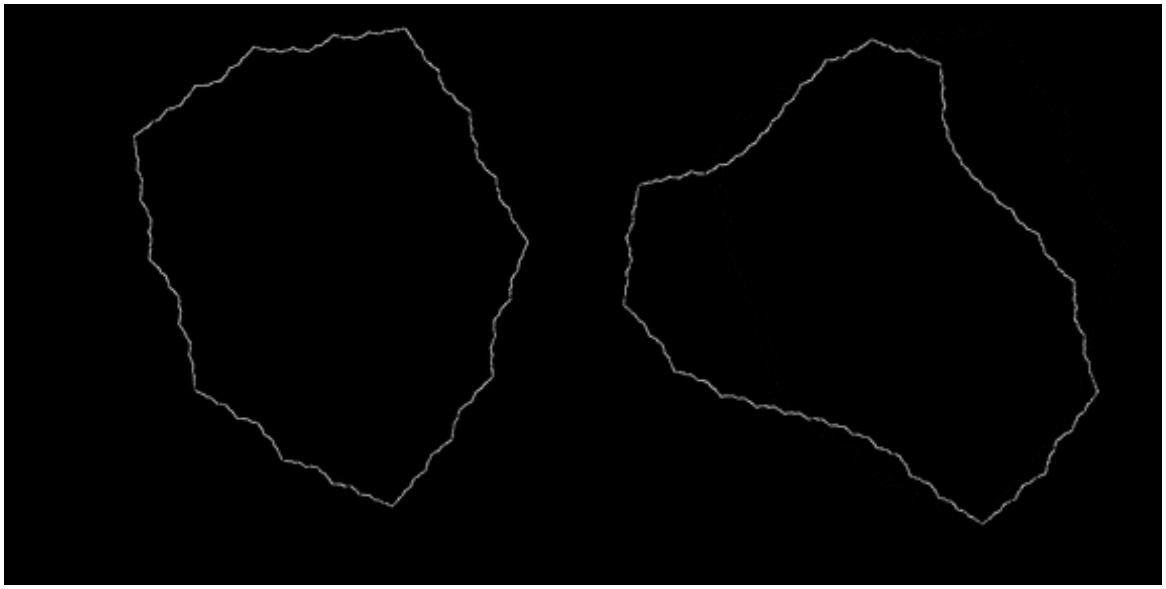

Fig. 4. Infolding Siegel disc near 1/3. One can see virtual Siegel disc

This is sketched in Fig. 1 representing a multiple beam interference image of living sarcoma cells in a tissue culture in air (magnification: 1.000). Optically identical regions are presented as light and dark elliptical zones which together form a topographic map of the cell. The cell thickness, shape and intramembranous volume can be easily calculated from the interference pattern.

In accordance with the modern standards the above method may seem to provide insufficient resolution and low information. However, there are still no mathematical approximations of intermembrane interference patterns, different from the ones derivable from the first physical principles. We propose here to apply Julia sets and Fatou components, such as Herman ring and Siegel disc for approximating carcinoma cells. The definition of Siegel disc is provided in the Table 1. Fig. 2 (compare with Fig. 1) shows an example of such an approach application, representing the early iterations of a fractal Julia set with a Siegel disc and an "isosurface-like" ("equipotential line – like") visualization of this filled Julia set for the golden mean rotation number with the Siegel disc and some orbits inside. It can be seen that Fig. 2 satisfactory simulates the morphology from Fig. 1. Thus, there is an appropriate approximation for this morphology due to the membranous properties of the cell represented here formally using Fatou components. A similar visualization can be obtained using the Herman ring, but this is beyond the scope of this report for the lack of space. The morphology of cells with filopodia also may6 be approximated by Siegel disc formalism, including dynamic representation (see Fig. 3 – “Infolding Siegel disc near 2/7” and Fig. 4 – “Infolding Siegel disc near 1/3”).

Table 1. Definition of Siegel disc

Definition of Siegel disks

Setting

$0 \in U$ open subset of $\mathbb{C}$
$f : U \to \mathbb{C}$ holomorphic

f defines a dynamical system: $z_{n+1} = f(z_n)$

$f(0) = 0$ (the origin is a fixed point)
the multiplier $f'(0)$ has modulus one: $f'(0) = e^{2i\pi\theta}$
the multiplier is aperiodic: $\theta \notin \mathbb{Q}$

This is called an
irrationally indifferent fixed point of a complex one dimensional holomorphic dynamical system.

What would it mean to behave like a rotation? That near 0,

- f is analytically conjugated to $R_\theta : z \mapsto e^{2i\pi\theta}z$? (meaning $\exists\phi$ analytic bijection defined near 0 mapping 0 to 0 and $\phi \circ f \circ \phi^{-1} = R_\theta$)
- f is topologically conjugated to R_θ? (now ϕ is only required to be a homeomorphism)
- the orbits stay bounded? (Lyapunov stability)

It turns out that all three are equivalent. We say that f is *linearizable*.

The quantity θ is unique and is called the *rotation number*.

https://www.math.univ-toulouse.fr/~cheritat/Exposes/Rome.pdf

5. Supplements: Possible program codes from the open access I-net sources

The Julia set is the set of complex numbers z that do not diverge under the following iteration:

z=z2+cz=z2+c

Where c is a constant complex number.

Different values of z reach infinity at different rates. A colourful fractal is produced by colouring the complex plane based on the number of iterations required to reach infinity.

```
function colour = julia(c, total_iterations, image_size, limits)
% Calculates julia set by iterating z = z^2 + c, where z and c are complex,
% and recording when z reaches infinity.
%
% Inputs:
%
% c                 Fixed complex number, of form a + bi
% total_iterations  Number of iterations of z = z^2 + c
% image_size        2D vector with number of complex coordinates in
```

```
%                   x and y directions
%  limits           Vector with 4 elements: min x, max x, min y, max y
%
%  Outputs:
%
%  colour           Matrix of doubles, with size equal to image_size.
%                   Plotting this matrix will produce a julia set


im_step = (limits(4) - limits(3)) / (image_size(2) - 1);
re_step = (limits(2) - limits(1)) / (image_size(1) - 1);

reals = limits(1) : re_step : limits(2);          % Real numbers
imags = limits(3) : im_step : limits(4);          % Imaginary numbers
z = bsxfun(@plus, reals(:), (imags(:) * 1i)');    % Complex coordinates
colour = inf(size(z));                            % Colour of Julia set

for iteration = 1:total_iterations
   index = isinf(z);
   % Only perform calculation on the z values that are less than infinity
   z(~index) = z(~index).^2 + c;
   % Colour depends on number of iterations to reach infinity
   colour(index & isinf(colour)) = iteration;
end

colour = colour'; % Transpose so that plot will have reals on the x axis

end
```

https://codereview.stackexchange.com/questions/145752/function-for-plotting-julia-set

```
function Julia(c,k,v)

% JULIA(C,K,V) draws the Julia set with the following parameters:
% c is a complex number used in the map f(z) = z² + c.
% k gives the number of iterations
% v determines the number of points on the x-axis.

% JULIA uses c = 0.2+0.65i, k = 14, v = 500.

% This file was generated by students as a partial fulfillment
% for the requirements of the course "Fractals", Winter term
% 2004/2005, Stuttgart University.

% Author : Sylvia Frey
% Date   : Nov 2004
% Version: 1.1

% default settings
if nargin < 3
   c = 0.2+0.65i;
   k = 14;
   v = 500;
end

% radius of the circle beyond which every point diverges
r = max(abs(c),2);
```

```
% divide the x-axis
d = linspace(-r,r,v);

% create the matrix A containing complex numbers
A = ones(v,1)*d+i*(ones(v,1)*d)';

% create the point matrix
B = zeros(v,v);

% iteration
for s = 1:k
   B = B+(abs(A)<=r);
   % the map
   A = A.*A+ones(v,v).*c;
end;

% plot settings
imagesc(B);
colormap(jet);

hold off;
axis equal;
axis off;
```

http://m2matlabdb.ma.tum.de/download.jsp?MC_ID=5&SC_ID=13&MP_ID=283

Julia(c,k,v) draws the Julia set with the following parameters:
c is a complex number used in the map f(z) = z^2 + c.
k gives the number of iterations.
v determines the number of points on the x-axis.

Julia uses c = 0.2+0.65i, k = 14, v = 500.

This file was generated by students as a partial fulfillment
for the requirements of the course "Fractals",
Winter term 2004/2005, Stuttgart University.

Visualize Julia Sets using Matlab

```
function myjulia(Zmax,c,N)
% Generate and visualize quadratic Julia Sets
% More information about Julia Sets can be found here:
% http://en.wikipedia.org/wiki/Julia_set
% this code is for the assignment of the "Introduction to Matlab" offered
by MITOPENCOURSEWARE
% Coded by http://scriptdemo.blogspot.com

if (nargin==1)
  Ndemo=Zmax; clear Zmax
  switch Ndemo
  case {1}
     myjulia(1,-0.297491+i*0.641051,100);
     return;
  case {2}
     myjulia(0.35,-0.297491+i*0.641051,250);
     return;
  otherwise
    disp('Not defined demo type!')
    help myjulia;
    return
  end
```

```
elseif (nargin~=3)
  help myjulia;
  return
end

% generate the basic matrix
NM=500;
[Z,tmpy]=meshgrid(linspace(-Zmax,Zmax,NM),zeros(1,NM));
Z=Z+i*Z'; clear tmpy

% compute the escape velocity
myM=reshape(escapeVelocity(Z(:),c,N),NM,NM);

% visualize the results
imagesc(atan(0.1*myM)); figurenicer;axis xy;

function n=escapeVelocity(z0,c,N)
n=z0*0;
NLen=length(z0);
IndZ=1:length(z0);
IndZ=IndZ';
for ni=1:N
    IndLT=find(abs(z0)<2);
    IndGE=find(abs(z0)>=2);
    n(IndZ(IndGE))=ni;
    if (length(IndLT)>0)
      z0(IndLT)=z0(IndLT).*z0(IndLT)+c;
    end
    z0(IndGE)=[];
    IndZ(IndGE)=[];
end
if ~isempty(IndZ)
  n(IndZ)=N;
end
```

Basin of attraction to infinity = exterior of filled-in Julia set and The Divergence Scheme = Escape Time Method (ETM)

First read definitions

Here one computes *forward iterations* of a complex point Z_0:

Here is function which computes the *last iteration*, that is the first iteration that lands in the target set (for example leaves a circle around the origin with a given *escape radius* ER) for the iteration of the complex quadratic polynomial above. It is a iteration (integer) for which (abs(Z)>ER). It can also be improved [2]

C version (here ER2=ER*ER) using double floating point numbers (without complex type numbers):

```
int GiveLastIteration(double Zx, double Zy, double Cx, double Cy, int IterationMax, int ER2)
{
 double Zx2, Zy2; /* Zx2=Zx*Zx;  Zy2=Zy*Zy  */
 int i=0;
 Zx2=Zx*Zx;
 Zy2=Zy*Zy;
 while (i<IterationMax && (Zx2+Zy2<ER2) ) /* ER2=ER*ER */
 {
```

```
  Zy=2*Zx*Zy + Cy;
  Zx=Zx2-Zy2 +Cx;
  Zx2=Zx*Zx;
  Zy2=Zy*Zy;
  i+=1;
 }
 return i;
}
```

C with complex type from GSL :[3]

```
#include <gsl/gsl_complex.h>
#include <gsl/gsl_complex_math.h>
#include <stdio.h>
// gcc -L/usr/lib -lgsl -lgslcblas -lm t.c
// function fc(z) = z*z+c

gsl_complex f(gsl_complex z, gsl_complex c) {
 return gsl_complex_add(c, gsl_complex_mul(z,z));
}

int main () {
 gsl_complex c = gsl_complex_rect(0.123, 0.125);
 gsl_complex z = gsl_complex_rect(0.0, 0.0);
 int i;
 for (i = 0; i < 10; i++) {
  z = f(z, c);
  double zx = GSL_REAL(z);
  double zy = GSL_IMAG(z);
  printf("Real: %f4 Imag: %f4\n", zx, zy);
 }
 return 0;
}
```

C++ versions:

```
int GiveLastIteration(complex C,complex Z , int imax, int ER)
{
 int i; // iteration number
 for(i=0;i<=imax-1;i++) // forward iteration
  {
   Z=Z*Z+C; // overloading of operators
   if(abs(Z)>ER) break;
  }
 return i;
}
#include <complex> // C++ complex library

// bailout2 = bailout * bailout
// this function is based on function esctime from mndlbrot.cpp
// from program mandel ver. 5.3 by Wolf Jung
// http://www.mndynamics.com/indexp.html

int escape_time(complex<double> Z, complex<double> C , int iter_max,  double bailout2)
```

```
{
 // z= x+ y*i   z0=0
 long double x =Z.real(), y =Z.imag(),  u ,  v ;
 int iter; // iteration
 for ( iter = 0; iter <= iter_max-1; iter++)
 { u = x*x;
   v = y*y;
   if ( u + v <= bailout2 )
     {
       y = 2 * x * y + C.imag();
       x = u - v + C.real();
     } // if
   else break;
 } // for
 return iter;
} // escape_time
```

[4]

Delphi version (using user defined complex type, cabs and f functions)

```
function GiveLastIteration(z,c:Complex;ER:real;iMax:integer):integer;
 var i:integer;
 begin
 i:=0;
 while (cabs(z)<ER) and (i<iMax) do
   begin
     z:= f(z,c);
     inc(i);
   end;
 result := i;
end;
```

where :

```
type complex = record x, y: real; end;

function cabs(z:complex):real;
begin
 cabs:=sqrt(z.x*z.x+z.y*z.y)
end;

function f(z,c:complex):complex; // complex quadratic polynomial
 var tmp:complex;
begin
 tmp.x := (z.x*z.x) - (z.y*z.y) + c.x;
 tmp.y := 2*z.x*z.y + c.y ;
 result := tmp;

end;
```

Delphi version without explicit definition of complex numbers :

```
function GiveLastIteration(zx0,zy0,cx,cy,ER2:extended;iMax:integer):integer;
 // iteration of z=zx+zy*i under fc(z)=z*z+c
 // where c=cx+cy*i
```

```
 // until abs(z)<ER  ( ER2=ER*ER )  or i>=iMax
 var i:integer;
    zx,zy,
    zx2,zy2:extended;
 begin
 zx:=zx0;
 zy:=zy0;
 zx2:=zx*zx;
 zy2:=zy*zy;

 i:=0;
 while (zx2+zy2<ER2) and (i<iMax) do
  begin
    zy:=2*zx*zy + cy;
    zx:=zx2-zy2 +cx;
    zx2:=zx*zx;
    zy2:=zy*zy;
    //
    inc(i);
  end;
 result := i;
end;
```

Euler version by R. Grothmann (with small change : from z^2-c to z^2+c) [5]

```
function iter (z,c,n=100) ...

h=z;
loop 1 to n;
h=h^2 + c;
if totalmax(abs(h))>1e20; m=#; break; endif;
end;
return {h,m};
endfunction
```

Lisp version
This version uses complex numbers. It makes the code short but is also inefficien.

```
((DEFUN GIVELASTITERATION (Z_0 _C IMAX ESCAPE_RADIUS)
  (SETQ Z Z_0)
  (SETQ I 0)
  (LOOP WHILE (AND (< I IMAX) (< (ABS Z) ESCAPE_RADIUS)) DO
    (INCF I)
    (SETQ Z (+ (* Z Z) _C)))
   I)
```

Maxima version :

```
/* easy to read but very slow version, uses complex type numbers */
GiveLastIteration(z,c):=
 block([i:0],
  while abs(z)<ER and i<iMax
    do (z:z*z + c,i:i+1),
  i)$
/* faster version, without use of complex type numbers,
```

```
  compare with c version, ER2=ER*ER */
GiveLastIter(zx,zy,cx,cy,ER2,iMax):=
block(
 [i:0,zx2,zy2],
 zx2:zx*zx,
 zy2:zy*zy,
 while (zx2+zy2<ER2) and i<iMax do
 (
  zy:2*zx*zy + cy,
  zx:zx2-zy2 +cx,
  zx2:zx*zx,
  zy2:zy*zy,
  i:i+1
 ),
 return(i)
);
```

Boolean Escape time [edit]

Algorithm: for every point z of dynamical plane (z-plane) compute iteration number (last iteration) for which magnitude of z is greater than escape radius. If last_iteration=max_iteration then point is in filled-in Julia set, else it is in its complement (attractive basin of infinity). Here one has 2 options, so it is named boolean algorithm.

```
if (LastIteration==IterationMax)
   then color=BLACK;   /* bounded orbits = Filled-in Julia set */
   else color=WHITE;  /* unbounded orbits = exterior of Filled-in Julia set  */
```

In theory this method is for drawing Filled-in Julia set and its complement (exterior), but when c is Misiurewicz point (Filled-in Julia set has no interior) this method draws nothing. For example for c=i . It means that it is good for drawing interior of Filled-in Julia set.

ASCII graphic*[edit]*

```
; common lisp
(loop for y from -2 to 2 by 0.05 do
    (loop for x from -2 to 2 by 0.025 do
                (let* ((z (complex x y))
                (c (complex -1 0))
                (iMax 20)
                        (i 0))

                (loop       while (< i iMax ) do
                        (setq z (+ (* z z) c))
                        (incf i)
                        (when (> (abs z) 2) (return i)))


        (if (= i iMax) (princ (code-char 42)) (princ (code-char 32)))))
    (format t "~%"))
```

Source: https://en.wikibooks.org/wiki/Fractals/Iterations_in_the_complex_plane/Julia_set

References

Abdelsalam et al., 2010 – *Abdelsalam, D.G., Shaalan, M.S., Eloker, M.M.* (2010). Surface microtopography measurement of a standard flat surface by multiple-beam interference fringes at reflection. *Optics and Lasers in Engineering*, 48(5): 543-547.

Ackerman, 1979 – *Ackerman, A.B.* (1979). Subtle clues to diagnosis by conventional microscopy: The patch stage of Kaposi's sarcoma. *The American Journal of Dermatopathology*, 1(2): 165-172.

Åkerman et al., 1988 – *Åkerman, M., Alvegård, T., Eliasson, J., Garwicz, S., Mandahl, N., Rydholm, A., Willén, H.* (1988). A case of Ewing's sarcoma diagnosed by fine needle aspiration: Light microscopy, electron microscopy and chromosomal analysis. *Acta Orthopaedica Scandinavica*, 59(5): 589-592.

Altenburg et al., 1976 – *Altenburg, B.C., Via, D.P., Steiner, S.H.* (1976). Modification of the phenotype of murine sarcoma virus-transformed cells by sodium butyrate: effects on morphology and cytoskeletal elements. *Experimental cell research*, 102(2): 223-231.

Amazon, Rywlin, 1979 – *Amazon, K., Rywlin, A.M.* (1979). Subtle clues to diagnosis by conventional microscopy: Lymph node involvement in Kaposi's sarcoma. *The American Journal of Dermatopathology*, 1(2): 173-176.

Aoki et al., 1973 – *Aoki, T., Stephenson, J.R., Aaronson, S.A.* (1973). Demonstration of a cell-surface antigen associated with murine sarcoma virus by immunoelectron microscopy. *Proceedings of the National Academy of Sciences*, 70(3): 742-746.

Babacan et al., 2011 – *Babacan, S.D., Wang, Z., Do, M., Popescu, G.* (2011). Cell imaging beyond the diffraction limit using sparse deconvolution spatial light interference microscopy. *Biomedical optics express*, 2(7): 1815-1827.

Barakat, Abouzakhm, 1965 – *Barakat, N., Abouzakhm, F.G. (*1965). Phase modulation of the first beam in reflected multiple beam interference fringes. *Optica Acta: International Journal of Optics*, 12(4): 321-332.

Barakat et al., 1965 – *Barakat, N., Farghaly, A.S., Abd-El-Azim, A.* (1965). Studies on multiple beam interference fringes formed on high order planes of localization: intensity distribution and the fringe shift between successive planes of localization. *Optica Acta: International Journal of Optics*, 12(2): 205-212.

Barakat et al., 1985 – *Barakat, N., Hamza, A.A., Goneid, A.S.* (1985). Multiple-beam interference fringes applied to GRIN optical waveguides to determine fiber characteristics. *Applied optics*, *24*(24), 4383-4386.

Barakat et al., 1988 – Barakat, N., El-Hennawi, H. A., & El-Diasti, F. (1988). Multiple-beam interference fringes applied to GRIN optical waveguides to examine fiber formation. *Applied optics*, 27(24): 5090-5094.

Barakat et al., 2001 – *Barakat, N., El-Hennawi, H.A., El-Ghafar, E. A., El-Ghandoor, H., Hassan, R., El-Diasty, F.* (2001). Three-dimensional refractive index profile of a GRIN optical waveguide using multiple beam interference fringes. *Optics communications*, 191(1-2): 39-47.

Barer, Joseph, 1957 – *Barer, R., Joseph, S.* (1957). Phase-contrast and interference microscopy in the study of cell structure. *Symp. Soc. exp. Biol.*, 10: 160-184.

Baumbach et al., 1989 – *Baumbach, P., Rassow, B., Wesemann, W.* (1989). Absolute ocular fundus dimensions measured by multiple-beam interference fringes. *Investigative ophthalmology & visual science*, 30(11): 2314-2319.

Becker et al., 1991 – *Becker, J., Schuppan, D., Rabanus, J. P., Gelderblom, H. R., Reichart, P.* (1991). Immunoelectron microscopy shows an atypical pattern and a quantitative shift of collagens type I, III and VI in oral Kaposi's sarcoma of AIDS. *Virchows Archiv A*, 419(3): 237-244.

Beziat et al., 1989 – *Beziat, J.L., Tabone, E., Bailly, C., Gerard, J.P.* (1989). Osteogenic sarcoma of the tongue: case report with light and electron microscopy studies and review of the literature. *Journal of Oral and Maxillofacial Surgery*, 47(5): 524-528.

Bhardwaj et al., 2017 – *Bhardwaj, R., Saxena, S.B., Sharma, P., Jaiswal, V.K., Mehrotra, R.* (2017). Experimental realisation of parallel optical logic gates and combinational logic using multiple beam interference. *Optik – International Journal for Light and Electron Optics*, 128: 253-263.

Boutelje, 1972 – *Boutelje, B.* (1972). Calculation of lignin concentration and porosity of cell-wall regions by interference microscopy. *Svensk Papperstidning-Nordisk Cellulosa*, 75(16): 683.

Braun, Fromherz, 1997 – *Braun, D., Fromherz, P.* (1997). Fluorescence interference-contrast microscopy of cell adhesion on oxidized silicon. *Applied Physics A: Materials Science & Processing*, 65(4): 341-348.

Brazhe et al., 2008 – *Brazhe, A.R., Brazhe, N.A., Maksimov, G.V., Ignatyev, P.S., Rubin, A.B., Mosekilde, E., Sosnovtseva, O.V.* (2008). Phase-modulation laser interference microscopy: an advance in cell imaging and dynamics study. *Journal of biomedical optics*, 13(3): 034004.

Briggs et al., 2006 – *Briggs, J.A., Johnson, M.C., Simon, M.N., Fuller, S.D., Vogt, V.M.* (2006). Cryo-electron microscopy reveals conserved and divergent features of gag packing in immature particles of Rous sarcoma virus and human immunodeficiency virus. *Journal of molecular biology*, 355(1): 157-168.

Brossel, 1946 – *Brossel, J.* (1946). Asymmetrical Broadening with Multiple-Beam Interference Fringes. *Nature*, 157(3993): 623.

Bruce, 1951 – *Bruce, C.F.* (1951). Transmission-like Multiple-Beam Reflexion Interference Fringes. *Nature*, 167(4245): 398.

Burnett, 1965 – *Burnett, C.* (1965). Instructional use of multiple-beam located interference fringes. *American Journal of Physics*, 33(1): 67.

Chaturvedi, 2013 – *Chaturvedi, A.* (2013). Molecular dissection of the mechanism utilized by the EWS/FLI oncogene to influence the morphology and behavior of Ewing sarcoma cells (Doctoral dissertation, The University of Utah).

Chernyaev et al., 2008 – *Chernyaev, I., Suvorova, A., Podgornov, F., Haase, W.* (2008). Influence of the multiple beam interference on phase retardation of liquid crystal cells. *Molecular Crystals and Liquid Crystals*, 488(1): 219-230.

Choux et al., 1981 – *Choux, R., Pluot, M., Faugere, M. C., Rodriguez, M., Hassoun, J., Caulet, T.* (1981). Clear cell sarcoma of the tendons and aponeuroses. A study of 2 cases using electron microscopy. *La semaine des hopitaux: organe fonde par l'Association d'enseignement medical des hopitaux de Paris*, 57(9-10): 479-482.

Civitelli et al., 1992 – *Civitelli, R., Fujimori, A., Bernier, S.M., Warlow, P.M., Goltzman, D., Hruska, K.A., Avioli, L.V.* (1992). Heterogeneous intracellular free calcium responses to parathyroid hormone correlate with morphology and receptor distribution in osteogenic sarcoma cells. *Endocrinology*, 130(4): 2392-2400.

Courington and Vogt, 1967 – *Courington, D., Vogt, P.K.* (1967). Electron microscopy of chick fibroblasts infected by defective Rous sarcoma virus and its helper. *Journal of virology*, *1*(2): 400-414.

Donaldson, 1985 – *Donaldson, L.A.* (1985). Critical assessment of interference microscopy as a technique for measuring lignin distribution in cell walls. *NZJ For. Sci*, 15: 349-360.

Dorfman, 1962 – *Dorfman, R.F.* (1962). Enzyme histochemistry and fluorescence microscopy of Kaposi's sarcoma, malignant hemangioendothelioma, and postmastectomy lymphangiosarcoma. *S. Afr. med. J*, 36: 989-990.

Drazba et al., 1997 – *Drazba, J., Liljelund, P., Smith, C., Payne, R., Lemmon, V.* (1997). Growth cone interactions with purified cell and substrate adhesion molecules visualized by interference reflection microscopy. *Developmental brain research*, 100(2): 183-197.

Driessens et al., 1964 – *Driessens, J., Dupont, A., Demaille, A., Puvion, E.* (1964). Cytological study by electron microscopy of the rat jensen sarcoma. *Comptes rendus des seances de la Societe de biologie et de ses filiales*, 158: 559.

Dunn, Zicha, 1993 – *Dunn, G.A., Zicha, D.* (1993). Phase-shifting interference microscopy applied to the analysis of cell behaviour. *Symposia of the Society for Experimental Biology*, 47: 91-106.

Dunn, Zicha, 1994 – *Dunn, G.A., Zicha, D.* (1994). Using interference microscopy to study cell behaviour. *Handbook of Cell Biology*, 25-33.

Earle, 1975 – *Earle, W.R.* (1975). The Development of Variations in Transplantability and Morphology Within a Clone of Mouse Fibroblasts Transformed to Sarcoma-Producing Cells In *Vitro1. Readings in Mammalian Cell Culture*: 185.

El-Dehemy et al., 1981 – *El-Dehemy, K.A., El-Nicklawy, M.M., Hassan, A.F., Nasr, E.A.* (1981). Studies on the visibility and intensity distribution of multiple-beam interference fringes. *Acta Physica Polonica: A*, 60: 389.

El-Diastry, 2001 – *El-Diasty, F.* (2001). Theory and measurement of Young's modulus radial profiles of bent single-mode optical fibers with the multiple-beam interference technique. *JOSA A*, 18(5): 1171-1175.

El-Hennawi et al., 2012 – *El-Hennawi, H.A., El-Diasty, F., El-Ghandoor, H., Soliman, M.A.* (2012). Multiple-beam interference fringes applied to investigate the index profile of the optical fiber dip. *Optical and Quantum Electronics*, 43(1-5): 35-48.

Fabrizio, Cottrell, 1972 – *Fabrizio, A., Cottrell, J.* (1972, January). Light and electron-microscopy studies of fabrizio hamster reticulum-cell sarcoma. *American Journal of Patholog,* 66(3): A98.

Falimirski et al., 2007 – *Falimirski, M., Syed, A., Prybilla, D.* (2007). Immunocompetence of the severely injured spleen verified by differential interference contrast microscopy: the red blood cell pit test. *Journal of Trauma and Acute Care Surgery*, 63(5): 1087-1092.

Faust, 1952 – *Faust, R.C.* (1952). Multiple-beam interference microscopy. *Proc. R. Soc. Lond. A*, 211(1105): 240-254.

Fj et al., 1975 – *Fj, P.M., Cañadell, J.M., Herranz, P., Imizcoz, J.L., Vázquez, J.J.* (1975). Chordoid sarcoma of the femur. Electronic and optical microscopy study of a case. *Revista de medicina de la Universidad de Navarra*, 19(1): 133-141.

Fu et al., 2016 – *Fu, H.L., Mueller, J.L., Whitley, M.., Cardona, D.M., Willett, R.M., Kirsch, D.G., Brown J.Q., Ramanujam, N.* (2016). Structured illumination microscopy and a quantitative image analysis for the detection of positive margins in a pre-clinical genetically engineered mouse model of sarcoma. *PloS one*, 11(1): e0147006.

Fulinska, 1966 – *Fulinska, K.F.* (1966). Effect of the Asymmetry of the Interference Layer on the Contrast of Fizeau Fringes Produced by Multiple-Beam Interference in Reflected Light. *Optics and Spectroscopy*, 20: 495.

Gandzii, 1956 – *Gandzii, G.* (1956). Electron microscopy of cells from tissue cultures of chicken sarcoma. *Voprosy onkologii*, 2(2): 205-211.

Geissinger, Bond, 1971 – *Geissinger, H.D., Bond, E.F.* (1971). Nomarski differential interference contrast microscopy and scanning electron microscopy of tissue sections and fibroblast cell culture monolayers. *Mikroskopie*, 27(1): 32.

Geissinger, Duitschaever, 1971 – *Geissinger, H.D., Duitschaever, C.L.* (1971). Nomarski differential-interference contrast microscopy in transillumination : Its use on unstained or stained sections, smears, and wet mounts, or on fluorochromed sections and cell-culture monolayers. *Journal of Microscopy*, 94(2): 107-124.

Gingell, Todd, 1979 – *Gingell, D., Todd, I.* (1979). Interference reflection microscopy. A quantitative theory for image interpretation and its application to cell-substratum separation measurement. *Biophysical Journal*, 26(3): 507-526.

Gingell, 1982 – *Gingell, D, Todd, I., Owens, N.* (1982). Interaction between intracellular vacuoles and the cell surface analysed by finite aperture theory interference reflection microscopy. *Journal of cell science*, 54(1): 287-298.

Glauert, 1951 – *Glauert, A.M.* (1951). Superposition Effects in Multiple-Beam Interference Fringes. *Nature*, 168: 861-862.

Goldacre et al., 1957 – *Goldacre, R.J., Easty, D.M., Ambrose, E.J.* (1957). A cell compressor for the measurement of mass and concentration by interference microscopy. *Nature*, 180(4600): 1487.

Grazziotin et al., 2010 – *Grazziotin, T.C., Cota, C., Buffon, R.B., Pinto, L.A., Latini, A., Ardigò, M.* (2010). Preliminary evaluation of in vivo reflectance confocal microscopy features of Kaposi's sarcoma. *Dermatology*, *220*(4), 346-354.

Guntaka et al., 1976 – *Guntaka, R.V., Richards, O.C., Shank, P.R., Kung, H.J., Davidson, N., Pritsch, E., Bishop M.J., Varmus, H.E.* (1976). Covalently closed circular DNA of avian sarcoma virus: purification from nuclei of infected quail tumor cells and measurement by electron microscopy and gel electrophoresis. *Journal of molecular biology*, 106(2): 337-357.

Haldar et al., 2011 – *Haldar, J.P., Wang, Z., Popescu, G., Liang, Z.P.* (2011). Deconvolved spatial light interference microscopy for live cell imaging. *Ieee Transactions on Biomedical Engineering*, 58(9): 2489-2497.

Hamza et al., 2010 – *Hamza, A.A., Sokkar, T.Z.N., El-Farahaty, K.A., Raslan, M.I.* (2010). Reconstruction of refractive indices distribution in 3D using a single pattern of multiple-beam interference fringes for online investigation of necking phenomenon. *Polymer Testing*, *29*(8): 1031-1040.

Hanaichi et al., 1975 – *Hanaichi, T., Kanotanaka, K., Tanaka, T.* (1975). Properties of a rat-adapted murine sarcoma-virus (moloney)-size determination by electron-microscopy. *Journal of Electron Microscopy*, 24(3): 204-204.

Hargreaves, 1963 – *Hargreaves, C.M.D.* (1963). Multiple-beam 'Transmission-like'Fizeau Fringes in the Reflexion Interference System. *Nature*, 197(4870): 890.

Herriott, 1965 – *Herriott, D.R.* (1965). Multiple-beam interference fringes at large plate spacing. *Journal of the Optical Society of America,* 55(5): 614.

Herriott, 1966 – *Herriott, D.R.* (1966). Long-path multiple-wavelength multiple-beam interference fringes. *Journal of the Optical Society of America,* 56(6): 719-721.

Hibino, Takatsuji, 2002 – *Hibino, K., Takatsuji, T.* (2002). Suppression of multiple-beam interference noise in testing an optical-parallel plate by wavelength-scanning interferometry. *Optical review*, 9(2): 60-65.

Hiraki et al., 1974 – *Hiraki, S., Chan, J.C., Hales, R.L., Dmochowski, L.* (1974). An immunoelectron microscopy study of Soehner-Dmochowski murine sarcoma virus following passage in rats and hamsters. *Cancer research*, 34(11): 2906-2910.

Hirst, 1961 – *Hirst, D.V.* (1961). Office examination of fresh cancer cells by interference phase microscopy. *American Journal of Obstetrics & Gynecology*, 81(1): 138-139.

Hodapp et al., 1952 – *Hodapp, E.L., Wade, N.J., Menz, L.J.* (1952). Survival, respiration and morphology of sarcoma-37 cells exposed to liquid nitrogen. *Proceedings of the Society for Experimental Biology and Medicine*, 81(2): 468-474.

Holt et al., 2008 – *Holt, M.R., Calle, Y., Sutton, D.H., Critchley, D.R., Jones, G.E., Dunn, G.A.* (2008). Quantifying cell–matrix adhesion dynamics in living cells using interference reflection microscopy. *Journal of microscopy*, *232*(1): 73-81.

Hou et al., 2016 – *Hou, Y., Wang, Z., Hu, Y., Li, D., Qiu, R.* (2016). Capture and sorting of multiple cells by polarization-controlled three-beam interference. *Journal of Optics*, 18(3): 035401.

Houston, 1974 – *Houston, T.* (1974). An Immunoelectron Microscopy Study of Soehner-Dmochowski Murine Sarcoma Virus following Passage in Rats and Hamsters'. *Cancer Research*, 34(2906â): 2910.

Husain, Nguyen, 1995 – *Husain, M., Nguyen, G.K.* (1995). Alveolar soft part sarcoma. Report of a case diagnosed by needle aspiration cytology and electron microscopy. *Acta cytologica*, 39(5): 951-954.

Joshi, Medina, 2000a – *Joshi, N.V., Medina, H.* (2000). Multiple beam interference confocal microscopy: tool for morphological investigation of a living spermatozoon. *Microscopy and Microanalysis*, 6(5): 471-477.

Joshi, Medina, 2000b – *Joshi, N.V., Medina, H.* (2000, May). Multiple beam interference confocal microscopy: a tool for morphological investigation of living cells and tissues. *Three-Dimensional and Multidimensional Microscopy: Image Acquisition Processing VII,* 3919: 86-92. International Society for Optics and Photonics.

Joshi et al., 2001 – *Joshi, N.V., Medina, H., Tucci, P.* (2001). Effect of an electric field on the motility of Entamoeba histolytica examined by multiple-beam interference microscopy. *Experimental parasitology*, 97(4): 179-185.

Joshi et al., 2004 – *Joshi N.V., Medina H., Barboza J.M., Colantuoni G., Quintero M.* (2004). Detection, imaging, and kinetics of sub-micron organelles of chondrocytes by multiple beam interference microscopy. *Three-Dimensional and Multidimensional Microscopy: Image Acquisition and Processing XI*. – International Society for Optics and Photonics, 5324: 145-151.

Kanaya et al., 1985 – *Kanaya, K., Baba, N., Kitagawa, Y., Mukai, M.* (1985). The digital structural analysis of human alveolar soft part sarcoma obtained by electron microscopy. *Micron and microscopica acta*, 16(1): 17-32.

Kato, Makino, 1962 – *Kato, H., Makino, S.* (1962, January). Phase microscopy study on effects of temperature and chemicals upon locomotion of tumor cells of MTK-sarcoma III of a rat. *Japanese Journal of Genetics,* 37(5): 393.

Kawauchi, 1995 – *Kawauchi, S.* (1995). The Utility of Immunoelectron Microscopy in Diagnosis of Small Round Cell Sarcoma of Soft Tissue. *Journal of Japanese Orthopaedic Association*, 69: S1001-S1001.

Kellie et al., 1986 – *Kellie, S., Patel, B., Mitchell, A., Critchley, D.R., Wigglesworth, N.M., Wyke, J.A.* (1986). Comparison of the relative importance of tyrosine-specific vinculin

phosphorylation and the loss of surface-associated fibronectin in the morphology of cells transformed by Rous sarcoma virus. *Journal of cell science*, 82(1): 129-142.

Keski-Oja et al., 1980 – *Keski-Oja, J., De Larco, J.E., Rapp, U.R., Todaro, G.J.* (1980). Murine sarcoma growth factors affect the growth and morphology of cultured mouse epithelial cells. *Journal of cellular physiology*, 104(1): 41-46.

King et al., 1983 – *King, C.A., Preston, T.M., Miller, R.H.* (1983). Cell-substrate interactions in amoeboid locomotion — A matched reflexion interference and transmission electron microscopy study. *Cell biology international reports*, 7(8): 641-649.

Kizilova et al., 2010 – *Kizilova, N.N., Tishko, T.V., Tishko, D.V.* (2010). Analysis of erythrocyte shape using digital holographic interferention microscopy. *3rd Eurasian Congress on Medical Physics and Engineering 'Medical Physics*, pp. 260-262.

Koniukhov, 1971 – *Koniukhov, V.* (1971). [Theory of a Fabry-Perot interferometer with a small wedge between the mirrors]. *Zhurnal Prikladnoi Spektroskopii*, 14: 212-215.

Koppelmann, Vosskuhl, 1973 – *Koppelmann, G., Vosskuhl, W.* (1973). Intensity distributions in multiple-beam fizeau interference fringes. 2. Experiments for normal incidence. *Optik*, 37(2): 164-174.

Koppelmann, 1972 – *Koppelmann, G.* (1972). Intensity distribution in multiple-beam fizeau interference fringes. 1. *Optik*, 36(4): 474.

Koppelmann, 1974 – *Koppelmann, G.* (1974). Intensity distributions in multiple-beam fizeau interference fringes. 3. Similarity relations for non-normal incidence. *Optik*, 40(1): 89-100.

Krischer et al., 1999 – *Krischer, J., Braun, R. P., Toutous-Trellu, L., Saurat, J. H., Pechere, M.* (1999). Kaposi's sarcoma: a new approach of lesional follow-up using epiluminescent light microscopy. *Dermatology (Basel, Switzerland)*, 198(4): 420-422.

Kubo et al., 1969 – *Kubo, T.* (1969). Clear cell sarcoma of patellar tendon studied by electron microscopy. *Cancer*, 24(5): 948-953.

Kukuté, Smirnova, 1981 – *Kukuté, B.G., Smirnova, E.A.* (1981). Electron microscopy in the differential diagnosis of uterine sarcoma. *Arkh. Pat.*, 43(7): 23-28.

Lee and Richards, 1964 – *Lee, H., Richards, V.* (1964). Relationship between radiation dose and giant cells in the surviving cell population of mouse marrow as determined by interference microscopy. *Nature*, 204(4959): 656.

Lee at al., 1960 – *Lee, H., Richards, V., Klausner, C.* (1960). Dry mass and cell area changes in Ehrlich mouse ascites carcinoma cells after complement-fixation reaction measured by interference microscopy. *Cancer research*, 20(10): 1415-1421.

Li et al., 2007 – *Li, H.W., McCloskey, M., He, Y., Yeung, E.S.* (2007). Real-time dynamics of label-free single mast cell granules revealed by differential interference contrast microscopy. *Analytical and bioanalytical chemistry*, 387(1): 63-69.

Limozin, Sengupta, 2009 – *Limozin, L., Sengupta, K.* (2009). Quantitative reflection interference contrast microscopy (RICM) in soft matter and cell adhesion. *ChemPhysChem*, 10(16): 2752-2768.

Llombart-Bosch, Peydro-Olaya, 1983 – *Llombart-Bosch, A., Peydro-Olaya, A.* (1983). Scanning and transmission electron microscopy of Ewing's sarcoma of bone (typical and atypical variants). *Virchows Archiv A*, 398(3): 329-346.

Ludford, Smiles, 1950 – *Ludford, R.J., Smiles, J.* (1950). Cytological characteristics of fibroblasts and sarcoma cells demonstrable by phase-contrast microscopy. *Journal of Microscopy*, 70(2): 186-193.

Luse, 1960 – *Luse, S.A.* (1960). A synovial sarcoma studied by electron microscopy. *Cancer*, *13*(2): 312-322.

Majeed et al., 2015 – *Majeed, H., Kandel, M. E., Han, K., Luo, Z., Macias, V., Tangella, K.V., Balla A., Popescu, G.* (2015). Breast cancer diagnosis using spatial light interference microscopy. *Journal of biomedical optics*, 20(11): 111210.

Majeed et al., 2016 – *Majeed, H., Nguyen, T., Macias, V., Tangella, K., Kajdacsy-Balla, A., Do, M., Popescu, G.* (2016). Towards Automated Histopathology of Breast Cancer Using Spatial Light Interference Microscopy (SLIM). *Laboratory Investigation*, 96: 55A-56A.

Marquart, 2006 – *Marquart, K.H.* (2006). Electron microscopy reveals fungal cells within tumor tissue from two African patients with AIDS-associated Kaposi sarcoma. *Ultrastructural pathology*, 30(3): 187-192.

Matsuzaki et al, 2016 – *Matsuzaki, T., Ito, K., Masuda, K., Kakinuma, E., Sakamoto, R., Iketaki, K., Tanii, T.* (2016). Quantitative evaluation of cancer cell adhesion to self-assembled monolayer-patterned substrates by reflection interference contrast microscopy. *The Journal of Physical Chemistry B*, 120(7): 1221-1227.

Mellors et al., 1953 – *Mellors R.C., Kupfer A., Hollender A.* (1953). Quantitative cytology and cytopathology. Measurement of the thickness, the volume, the hydrous mass, and the anhydrous mass of living cells by interference microscopy. *Cancer*. 1953 Mar; 6(2): 372-84.

Mellors, 1953 – *Mellors, R.C.* (1953). The quantitative analysis of the cell by interference and ultraviolet microscopy. *Texas reports on biology and medicine*, 11(4): 693-708.

Melors, 1953 – *Mellors, R.C.* (1953). Multiple beam interference microscopy and quantitative cytology. *Journal of the Optical Society of America*, 43(4): 326-326.

Melors, 1954 – *Mellors, R.C.* (1954). Photographic methods for the measurement of the organic mass of cells and cell components (including sets of chromosomes) by multiple beam interference microscopy. *Journal of Histochemistry & Cytochemistry*, 2(6): 482-483.

Miller, Dvorak, 1973 – *Miller, L.H., Dvorak, J.A.* (1973). Visualization of red cell membranes of lysed malaria-infected cells by differential interference microscopy. *Journal of Parasitology*, 59(1): 202-3.

Mitchell et al., 1978 – *Mitchell, W., Schuffman, S., Korinek, J., Moses, H.* (1978). Effect of cyclic-AMP on growth properties and surface morphology of XC sarcoma-cells in vitro. Preprint.

Mukai et al., 1983 – *Mukai, M., Iri, H., Nakajima, T., Hirose, S., Torikata, C., Kageyama, K., Ueno, N., Murakami, K.* (1983). Alveolar soft-part sarcoma. A review on its histogenesis and further studies based on electron microscopy, immunohistochemistry, and biochemistry. *The American journal of surgical pathology*, 7(7): 679-689.

Murti et al., 1981 – *Murti, K.G., Bondurant, M., Tereba, A.L.L.A.N.* (1981). Secondary structural features in the 70S RNAs of Moloney murine leukemia and Rous sarcoma viruses as observed by electron microscopy. *Journal of virology*, 37(1): 411-419.

Nanomuna, 1988 – *Nanomuna, A.* (1988). Primary artery sarcoma. Report of two cases and studied by immunohistochemistry and electric microscopy and a review of 110 cases in the literature. *Acta Pathol Jpn*, 38: 883-896.

Nishimi et al., 1961 – *Nishiumi, Y., Okano, H., Imai, T.* (1961). Inoculation of chicken sarcoma virus into chicken thymus. An electron microscopy. *Proceedings of the Society for Experimental Biology and Medicine*, 107(1): 88-90.

Nishio et al., 2003 – *Nishio, J., Iwasaki, H., Sakashita, N., Haraoka, S., Isayama, T., Naito, M., ..., Kikuchi, M.* (2003). Undifferentiated (embryonal) sarcoma of the liver in middle-aged adults: smooth muscle differentiation determined by immunohistochemistry and electron microscopy. *Human pathology*, 34(3): 246-252.

Nonomura et al., 1988 – *Nonomura, A., Kurumaya, H., Kono, N., Nakanuma, Y., Ohta, G., Terahata, S., ... , Nishino, T.* (1988). Primary pulmonary artery sarcoma. Report of two autopsy cases studied by immunohistochemistry and electron microscopy, and review of 110 cases reported in the literature. *Pathology International*, 38(7): 883-896.

Obara et al., 2013 – *Obara, B., Roberts, M.A., Armitage, J.P., Grau, V.* (2013). Bacterial cell identification in differential interference contrast microscopy images. *BMC bioinformatics*, 14(1): 134.

Oord et al., 1986 – *Oord, J., Wolf-Peeters, C., Vos, R., Thomas, J., Desmet, V.J.* (1986). Sarcoma arising from interdigitating reticulum cells: report of a case, studied with light and electron microscopy, and enzyme-and immunohistochemistry. *Histopathology*, 10(5): 509-523.

Orenstein et al., 1997 – *Orenstein, J.M., Alkan, S., Blauvelt, A., Jeang, K.T., Weinstein, M.D., Ganem, D., Herndier, B.* (1997). Visualization of human herpesvirus type 8 in Kaposi's sarcoma by light and transmission electron microscopy. *AIDS*, 11(5): F35-F45.

Paganelli et al., 2018 – *Paganelli, A., Bassoli, S., Roncati, L., Bigi, L., Ciardo, S., Pellacani, G.* (2018). Pseudo-Kaposi sarcoma: report of a case investigated by dermoscopy, reflectance confocal microscopy and optical coherence tomography. *Journal of the European Academy of Dermatology and Venereology*.

Pappelis et al., 1976 – *Pappelis, C.K., Slobin, J., Detwiler, H.D., Pappelis, A.J., Pappelis, G.A.* (1976). Comparison of buccal and nasal epithelial cells using a new cell development index and quantitative interference microscopy. *Acta cytologica*, 20(4): 372-374.

Paszek et al., 2012 – *Paszek, M.J., DuFort, C.C., Rubashkin, M.G., Davidson, M.W., Thorn, K.S., Liphardt, J.T., Weaver, V.M.* (2012). Scanning angle interference microscopy reveals cell dynamics at the nanoscale. *Nature methods*, 9(8): 825.

Pate et al., 1969 – *Patel, T.N., Braganca, B.M., Bellare, R.A.* (1969). Changes produced by cobra venom cytotoxin on the morphology of Yoshida sarcoma cells. *Experimental cell research*, 57(2-3): 289-297.

Pettinato et al., 1989 – *Pettinato, G., De, A. C., Insabato, L., Ferbo, U., Di, A. B., Marino, G.M.* (1989). Reactive glioma in intracranial sarcoma ('sarcoglioma'). Histology, electron microscopy and immunohistochemistry of two additional cases. *Applied pathology*, 7(3): 192-200.

Plowman et al., 2016 – *Plowman, R.S., Cassell, I., Ritland, F., Bonatus, T., Jorgensen, S.A., Towbin, A.J., Towbin, R.* (2016). Indolent synovial sarcoma in adolescent male: MR, PET, microscopy, and arthroscopy correlation. Applied Radiology – The Journal of Practical Medical Imaging and Management. [Electronic resource]. URL: https://appliedradiology.com/articles/indolent-synovial-sarcoma-in-adolescent-male-mr-pet-microscopy-and-arthroscopy-correlation

Popescu and Wang, 2012 – *Popescu, Gabriel, Zhuo Wang* (2012). Spatial light interference microscopy and fourier transform light scattering for cell and tissue characterization. U.S. Patent No. 8,184,298. 22 May 2012.

Prince, 1962 – *Prince, A.M.* (1962). Factors influencing the determination of cellular morphology in cells infected with Rous sarcoma virus. *Virology*, 18(4): 524-534.

Rice et al., 1973 – *Rice, R.W., Cabot, A., Johnston, A.D.* (1973). The application of electron microscopy to the diagnostic differentiation of Ewing's sarcoma and reticulum cell sarcoma of bone. *Clinical orthopaedics and related research*, 91: 174-185.

Richardson, 1972 – *Richardson, J.H.* (1972). Multiple-beam interference microscopy of metals by S. Tolansky. *Journal of Applied Crystallography*, 5(6): 442-442.

Roberge, Boivin, 1971 – *Roberge, R., Boivin, A.* (1971). Multiple-beam interference fringes formed by a spherical thin shell. *Journal of the Optical Society of America*, 61(11): 1561.

Roe, King, 1950 – *Roe, E.M.F., King, R.G.* (1950). Ultra-Violet Microscopy of Tumour and Virus of Rouse Fowl Sarcoma. *Phot. J.*, 90: 94.

Roy et al., 2006 – *Roy, M., Matsuda, K., Grover, C., Baldock, C.* (2006). Diffential Interference Phase Contrast Microscopy Using Multiple Beam Shearing Interferometry for Bio-imaging. *Australasian Physical & Engineering Sciences in Medicine*, 29(1): 157.

Said et al., 1997 – *Said, J.W., Chien, K., Tasaka, T., Koeffler, H. P.* (1997). Ultrastructural characterization of human herpesvirus 8 (Kaposi's sarcoma-associated herpesvirus) in Kaposi's sarcoma lesions: electron microscopy permits distinction from cytomegalovirus (CMV). *The Journal of Pathology: A Journal of the Pathological Society of Great Britain and Ireland*, 182(3): 273-281.

Salmeen et al., 1976 – *Salmeen, I.R.V.I.N.G., Rimai, L.A.J.O.S., Luftig, R.B., Libes, L., Retzel, E.R.N.E.S.T., Rich, M., McCormick, J.J.* (1976). Hydrodynamic diameters of murine mammary, Rous sarcoma, and feline leukemia RNA tumor viruses: studies by laser beat frequency light-scattering spectroscopy and electron microscopy. *Journal of virology*, 17(2): 584-596.

Salmon et al., 1998 – *Salmon, E.D., Yeh, E., Shaw, S., Skibbens, B., Bloom, K.* (1998). High-resolution video and digital-enhanced differential interference contrast light microscopy of cell division in budding yeast. *Methods in enzymology*, 298: 317-331.

Sandritter et al., 1960 – *Sandritter, W., Schiemer, H., Alt, W.* (1960). Interference microscopy in cytology and cancer research. *Klinische Wochenschrift*, 38: 590-595.

Schindl et al., 1995 – *Schindl, M., Wallraff, E., Deubzer, B., Witke, W., Gerisch, G., Sackmann, E.* (1995). Cell-substrate interactions and locomotion of Dictyostelium wild-type and mutants defective in three cytoskeletal proteins: a study using quantitative reflection interference contrast microscopy. *Biophysical Journal*, 68(3): 1177-1190.

Seegers et al., 1992 – *Seegers, J.C., Els, H.J.* (1992). Effects of gamma-linolenic acid on mitosis and nuclear morphology in osteogenic sarcoma cells. South African medical journal = Suid-Afrikaanse tydskrif vir geneeskunde, 81(9): 467-472.

Shaked et al., 2009 – *Shaked, N.T., Rinehart, M.T., Wax, A.* (2009). Dual-interference-channel quantitative-phase microscopy of live cell dynamics. *Optics letters*, 34(6): 767-769.

Shao-po, 1999 – *Shao-po, Z.* (1999). Experiment of multiple-beam equal inclination interference fringes. *Optical Technique*, (5): 82-90.

Siegler, 1970 – *Siegler, R.* (1970). Pathogenesis of virus-induced murine sarcoma. I. Light microscopy. *Journal of the National Cancer Institute*, 45(1): 135-147.

Smidová et al., 1968 – *Smidová, V., Ujházy, V., Matoska, J., Smida, J.* (1968). In vitro passages of hamster tumour cells induced with Schmidt-Ruppin strain of Rous sarcoma viruse: their oncogenicity, morphology and karyology. *Neoplasma*, 15(6): 597-605.

Smith, 1952 – *Smith, F.D.* (1952). Bright multiple beam interference fringes in reflection. *Journal of the Optical Society of America*, 42(11): 877-877.

Sosnovtseva et al., 2005 – *Sosnovtseva O.V., Pavlov A.N., Brazhe N.A., Brazhe A.R., Erokhova L.A., Maksimov G.V., Mosekilde E.* (2005). Interference microscopy under double-wavelet analysis: a new approach to studying cell dynamics. *Physical review letters*, 94(21): 218103.

Sun et al., 2008 – *Sun, W., Fang, N., Trewyn, B. G., Tsunoda, M., Slowing, I. I., Lin, V. S., Yeung, E. S.* (2008). Endocytosis of a single mesoporous silica nanoparticle into a human lung cancer cell observed by differential interference contrast microscopy. *Analytical and Bioanalytical Chemistry*, 391(6): 2119.

Sun et al., 2010 – *Sun, W., Fang, N., Trewyn, B. G., Tsunoda, M., Slowing, I. I., Lin, V. S., Yeung, E.S.* (2010). Endocytosis of single mesoporous silica nanoparticle into living human lung cancer cell (a549) observed by differential interference contrast microscopy. *Developing new optical imaging techniques for single particle and molecule tracking in live cells*, 38.

Svoboda, Hasek, 1956 – *Svoboda J., Hasek M.* (1956). Influencing the transplantability of the virus of Rous sarcoma by immunological approximation in turkeys. *Folia biol., Praha*, *2*: 256-284.

Tadmor et al., 2003 – *Tadmor, R., Chen, N., Israelachvili, J.N.* (2003). Thickness and refractive index measurements using multiple beam interference fringes (FECO). *Journal of colloid and interface science*, 264(2): 548-553.

Todd et al., 1988 – *Todd, I., Mellor, J. S., Gingell, D.* (1988). Mapping cell-glass contacts of Dictyostelium amoebae by total internal reflection aqueous fluorescence overcomes a basic ambiguity of interference reflection microscopy. *Journal of cell science*, 89(1): 107-114.

Tokuyama, Tokuyama, 1989 – *Tokuyama, H., Tokuyama, Y.* (1989). Bovine colostric transforming growth factor-β-like peptide that induces growth inhibition and changes in morphology of human osteogenic sarcoma cells (MG-63). *Cell Biology International Reports*, 13(3): 251-258.

Tolansky, Barakat, 1950 – *Tolansky, S., Barakat, N.* (1950). New Localized Multiple-Beam Interference Fringes formed with Curved Thin Sheets. *Proceedings of the Physical Society. Section B*, 63(8): 545.

Tolansky, Emara, 1955 – *Tolansky, S., Emara, S.H.* (1955). Precision multiple-beam interference fringes with high lateral microscopic resolution. *JOSA*, 45(10): 792-795.

Tolansky, 1945 – *Tolansky, S. (*1945). XXXI New contributions to interferometry. Part V. New multiple beam white light interference fringes and their applications. *The London, Edinburgh, and Dublin Philosophical Magazine and Journal of Science*, 36(255): 225-236.

Tolansky, 1970 – *Tolansky, S.* (1970). Multiple-beam interference microscopy of metals. Academic Press Inc. Ltd. Berkele, 147 p.

Tolansky, 1991 – *Tolansky, S.* (1991). New contributions to interferometry. V, New multiple beam white light interference fringes and their applications. *SPIE milestone series*, 28: 163-175.

Tolansky, 2000 – *Tolansky, S.* (2000). New Multiple Beam White Light Interference Fringes and their Applications. *SPIE milestone series*, 163: 246-255.

Tsokos et al., 1988 – *Tsokos, M., Miser, J., Horowitz, M., Kinsella, T., Balis, F., Triche, T.* (1988). Primitive round cell-sarcoma of bone-a group of tumors resembling ewings-sarcoma by light-microscopy, but with distinctive ultrastructural appearance. *Laboratory Investigation,* 58(1): A96.

Tsunoda et al., 2008 – *Tsunoda, M., Isailovic, D., Yeung, E.S.* (2008). Real-time three-dimensional imaging of cell division by differential interference contrast microscopy. *Journal of Microscopy*, 232(2): 207-211.

Tychinsky, Tikhonov, 2010 – *Tychinsky, V.P., Tikhonov, A.N.* (2010). Interference microscopy in cell biophysics. 1. Principles and methodological aspects of coherent phase microscopy. *Cell biochemistry and biophysics*, 58(3): 107-116.

Tychinsky, Tikhonov, 2010b – *Tychinsky, V.P., Tikhonov, A.N.* (2010). Interference microscopy in cell biophysics. 2. Visualization of individual cells and energy-transducing organelles. *Cell biochemistry and biophysics*, 58(3): 117-128.

Usson et al., 1997 – *Usson, Y., Guignandon, A., Laroche, N., Lafage-Proust, M. H., Vico, L.* (1997). Quantitation of cell-matrix adhesion using confocal image analysis of focal contact associated proteins and interference reflection microscopy. *Cytometry*, 28(4): 298-304.

Varela, Diazflores, 1977 – *Varela, J., Diazflores, L.* (1977). Epithelioid sarcoma-light and electron-microscopy observations. *Morfologia Normal y Patologica Seccion B – Anatomia Patologica*, 1(1): 117-121.

Verschueren, 1985 – *Verschueren, H.* (1985). Interference reflection microscopy in cell biology: methodology and applications. *Journal of Cell Science*, 75(1): 279-301.

Veselý, Pluta, 1972 – *Veselý, P., Pluta, M.* (1972). Indication of the surface location of refractive motile spots wreathing the central area of some tissue culture cells (rat Rous sarcoma cells, stereoscopic phase contrast microscopy). *Folia biologica*, 18(5): 374-375.

Vogt, Simon, 1999 – *Vogt, V.M., Simon, M.N.* (1999). Mass determination of Rous sarcoma virus virions by scanning transmission electron microscopy. *Journal of virology*, 73(8): 7050-7055.

Waldo et al., 1983 – *Waldo, E., Sidhu, G. S., Stahl, R., Zolla-Pazner, S.* (1983). Histiocytoid hemangioma with features of angiolymphoid hyperplasia and Kaposi's sarcoma. A study by light microscopy, electron microscopy, and immunologic techniques. *The American journal of dermatopathology*, 5(6): 525-538.

Waldo, 1979 – *Waldo, E.* (1979). Subtle clues to diagnosis by electron microscopy: Kaposi's sarcoma. *The American Journal of Dermatopathology*, 1(2): 177-182.

Wehland et al., 1979 – *Wehland, J., Osborn, M., Weber, K.* (1979). Cell-to-substratum contacts in living cells: a direct correlation between interference-reflexion and indirect-immuno-fluorescence microscopy using antibodies against actin and alpha-actinin. *Journal of cell science*, 37(1): 257-273.

Weinberger, Banfield, 1965 – *Weinberger, M.A., Banfield, W.G.* (1965). Fine structure of a transplantable reticulum cell sarcoma. I. Light and electron microscopy of viable and necrotic tumor cells. *Journal of the National Cancer Institute*, 34(4): 459-479.

Welch, et al., 1986 – *Welch, P., Grossi, C., Carroll, A., Dunham, W., Royal, S., Wilson, E., Crist, W.* (1986). Granulocytic sarcoma with an indolent course and destructive skeletal disease. Tumor characterization with immunologic markers, electron microscopy, cytochemistry, and cytogenetic studies. *Cancer*, 57(5): 1005-1010.

Yasuzumi et al., 1960 – *Yasuzumi, G., Sugihara, R., Nakano, S., Kise, T., Takeuchi, H.* (1960). Submicroscopic structure of cell necrobiosis of Yoshida sarcoma as revealed by electron microscopy. *Cancer research*, 20(3 Part 1): 339-343.

Yusipovich et al., 2011 – *Yusipovich, A.I., Zagubizhenko, M.V., Levin, G.G., Platonova, A., Parshina, E.Y., Grygorzcyk, R., Maksimov, G.V., Rubin, A.B., Orlov, S.N.* (2011). Laser interference microscopy of amphibian erythrocytes: impact of cell volume and refractive index. *Journal of microscopy*, 244(3): 223-229.

Zhudina, Shalumovich, 1969 – *Zhudina, A.I., Shalumovich, V.N.* (1969). Determination of nucleic acids in cells infected by Rous sarcoma virus by means of ultraviolet microscopy. *Voprosy onkologii*, 15(9): 74-79.